Preparation and characterization of PVDF/TiO$_2$ composite ultrafiltration membranes using mixed solvents

Maryam Tavakolmoghadam [1,2], Toraj Mohammadi [*1], and Mahmood Hemmati [2]

[1] *Research and Technology Centre for Membrane Processes, Faculty of Chemical Engineering,
Iran University of Science and Technology, Narmak, 16846, Tehran, Iran*
[2] *Research Institute of Petroleum Industry, Tehran, Iran*

Abstract.   To study the effect of titanium dioxide (TiO$_2$) nanoparticles on membrane performance and structure and to explore possible improvement of using mixed solvents in the casting solution, composite polyvinylidene fluoride (PVDF) ultrafiltration membranes were prepared via immersion precipitation method using a mixture of two solvents triethyl phosphate (TEP) and dimethylacetamide (DMAc) and addition of TiO$_2$ nanoparticles. Properties of the neat and composite membranes were characterized using scanning electron microscope (SEM), energy dispersive X-ray spectroscopy (EDS), Atomic force microscopy (AFM) and contact angle and membrane porosity measurements. The neat and composite membranes were further investigated in terms of BSA rejection and flux decline in cross flow filtration experiments. Following hydrophilicity improvement of the PVDF membrane by addition of 0.25 wt.% TiO$_2$, (from 70.53° to 60.5°) degree of flux decline due to irreversible fouling resistance of the composite membrane reduced significantly and the flux recovery ratio (FRR) of 96.85% was obtained. The results showed that using mixed solvents (DMAc/TEP) with lower content of TiO$_2$ nanoparticles (0.25 wt.%) affected the sedimentation rate of nanoparticles and consequently the distribution of nanoparticles in the casting solution and membrane formation which influenced the properties of the ultimate composite membranes.

Keywords: polyvinylidene fluoride; mixed solvents; immersion precipitation; titanium dioxide; ultrafiltration membrane

1. Introduction

Membrane technology has emerged as an advanced separation process almost in every industrial sector such as environmental, energy and chemical areas since the first commercial membrane was fabricated via phase inversion method in 1960s (Mulder 1996, Loeb and Sourirajan 1964). Phase inversion method has attracted great attention among researchers with regards to its simplicity and flexible production scales which helps to maintain low cost of production (Kesting 1985). This method could be employed in fabrication of a wide variety of polymeric membranes.

Among various membrane materials, polyvinylidene fluoride (PVDF) has received great attention due to its outstanding mechanical and physicochemical properties besides good thermal

---

∗Corresponding author, Professor, E-mail: torajmohammadi@iust.ac.ir

and chemical resistance to acid and basic cleaning (Liu *et al.* 2011, Razzaghi *et al.* 2014). Since early 1980s, which preparation of PVDF membranes had started, several methods have been employed for their fabrication, including phase inversion method. Phase inversion via immersion precipitation (IP) is the most commonly employed method in fabrication of the PVDF membranes (Liu *et al.* 2011). Immersion precipitation is a process where a polymer solution is cast on a suitable support, then immersed in a coagulation bath containing a non-solvent. Exchange of the solvent of the polymer solution and the non-solvent of the coagulation bath results in the phase separation (Mulder 1996, Guillen *et al.* 2011). A large part of the research and development of PVDF membranes prepared via immersion precipitation process has been focused on the effect of various preparation conditions on membrane morphology and performance, as well as the relationship between membrane structure with its formation process parameters (Liu *et al.* 2011, Zhang *et al.* 2012). Among many formation process parameters affecting polymer precipitation during phase inversion method, solvent plays a very important role in determining the ultimate membrane properties and performance. Proper selection of solvent leads to maintenance of the high polymer chain mobility and consequently formation of the uniform distribution of polymer configuration. Many researchers have investigated effect of solvent on PVDF membrane properties and performance. Bottino *et al*. (1988) identified eight organic solvents including N,N-dimethylacetamide (DMAc), N,N-dimethylformamide (DMF), N-methyl-2-pyrrolidon (NMP), dimethylsulfoxide (DMSO), hexamethylphosphoramide (HMPA), tetramethylurea (TMU), triethylphosphate (TEP) and trimethylphosphate (TMP) as good solvents for PVDF. They showed that by employing each type of these solvents, various structures of PVDF flat sheet membranes could be obtained (Bottino *et al.* 1991). Their experimental results demonstrated that the mechanism of PVDF membrane formation is governed by the kinetic factor, i.e., the mutual diffusivity between solvent and non-solvent, rather than their thermodynamic properties. Yeow *et al.* 2004 illustrated by SEM images that, by using TEP as solvent, a uniform sponge symmetric structure could be observed throughout the membrane cross-section using water as coagulant. Similar observations have been previously reported by Bottino *et al.* (1991) and Shih *et al.* (1990). The reason favoring formation of sponge-like structure of PVDF membrane using TEP as solvent is the relatively weak mutual affinity between TEP and water as non-solvent (Yeow *et al.* 2004). According to their SEM images, flat-sheet membranes cast with DMF and DMAc as solvents exhibited similar short finger like structures with sponge substrates indicating an instantaneous dimixing. Tao *et al.* (2013) discussed that relatively high permeability but low BSA rejection of the PVDF membranes prepared via phase inversion method using TEP as solvent, relates to the membrane polymorphism during phase inversion (Tao *et al.* 2013). They also concluded that PVDF/TEP/water casting solution has the potential to produce PVDF microfiltration (MF) membranes but some modifications are needed to improve their hydrophilicity, rejection and antifouling resistance. The reported values for permeabilities of PVDF membranes with pure DMAc as single solvent show low flux but distinctly high BSA rejection while these membranes suffer from low fouling resistance of the membranes due to their intrinsic hydrophobic properties (Liu *et al.* 2011, Song *et al.* 2012) and more shrinkage of the membranes (Teow *et al.* 2012).

Li *et al.* 2010 investigated effect of four different mixed solvents on membrane morphology and performance. Their results showed that the stronger solvent power of TMP-DMAc and TEP-DMAc results in faster precipitation rate and less membrane shrinkage and consequently higher water flux. The membrane cast from the latter system with TEP/DMAc ratio of 60/40, shows much shorter macrovoids beneath the skin layer, and this attributes to the higher rejection and the much better mechanical properties of the membrane.

In recent years, surface modification of polymeric membranes by incorporation of inorganic nanoparticles to make nanocomposite membranes has been proposed as an effective method to improve hydrophilicity and antifouling properties of the membranes (Kim and Van der Bruggen 2010, Bae and Tak 2005, Wang *et al.* 2013). Among different nanoparticles, titanium dioxide (TiO_2) has received much attention because of its stability, availability, and stronger chemical resistance to acids and bases compared to other metal oxides as well as its potential antifouling abilities (Zhang *et al.* 2013, Razmjou *et al.* 2012). There are two main approaches for fabrication of TiO_2 nanocomposite membranes: (1) blending the nanoparticles into the membrane (Song *et al.* 2012, Bae and Tak 2005, Cao *et al.* 2006, Damodar *et al.* 2009, Oh *et al.* 2009, Ngang *et al.* 2012, Li *et al.* 2013) and (2) coating the nanoparticles onto the surface of the membrane (Kim and Van der Bruggen 2010, Luo *et al.* 2005, Rahimpour *et al.* 2008, Shon *et al.* 2010, Damodar *et al.* 2012)

The incorporation of widely available commercial TiO_2 powders into polymeric membranes is one of the strategies to improve antifouling performance of the membranes. Compare to the coating approach, this method is simpler since the particles are added to the membrane casting solution. Many studies have investigated improvements of the PVDF membrane performance by TiO_2 blending (Song *et al.* 2012, Bae and Tak 2005, Cao *et al.* 2006, Damodar *et al.* 2009, Oh *et al.* 2009, Ngang *et al.* 2012, Rahimpour *et al.* 2011, Bian *et al.* 2011).

Generally, adding a well-chosen amount of TiO_2 nanoparticles to the casting solution may result in a thinner skin layer, a higher surface porosity of the skin layer and the higher permeability of membrane. However, a reduced permeability or a maximum permeability at intermediate nanoparticle loading has also been observed. Song *et al.* (2012) showed that water flux through PEG-TiO_2-doped PVDF membranes increases but the effect is concentration dependent: above a threshold concentration, water flux decreases and then increases again. As shown from their results when TiO_2 content increases from 0.25 wt.% to 0.5 wt.%, the membrane water flux decreases and pepsin rejection increases, However, when TiO_2 content increases from 0.5 wt.% to 2 wt.%, the membrane water flux increases and pepsin rejection decreases. Although the maximum water flux enhancement is obtained in this case at 2 wt.% TiO_2 content, a relatively high water flux with a better pepsin rejection is observed at low TiO_2 content of 0.25 wt.%. They interpreted that this effect is due to formation of some large pores on the membrane surface caused by TiO_2 nanoparticles agglomeration as reported in similar studies for other polymeric membrane Kim and Van der Bruggen (2010). While most of the researchers have used relatively high concentration of TiO_2 in PVDF matrix, Arsuaga *et al.* (2013) performed a similar study on PES with different nanoparticles to investigate the effectiveness of applying lower concentration of TiO_2. Wu *et al.* (2008), who observed a threshold value of 0.5 (wt.%) TiO_2 content showed that apart from a reduced permeability, a loss of mechanical strength may occur by further increasing the TiO_2 content. These somewhat contradictory results could also be observed in the reported values for contact angles, porosities and rejections. Differences may of course arise from differences in procedures and materials; nevertheless, it appears that the useful upper limit for the TiO_2 concentration is situated at lower concentrations than the values assumed by some researchers (Kim and Van der Bruggen 2010).

As shown in second row of Table 1, Damodar *et al.* (2009) prepared some modified PVDF membranes by adding different amounts of TiO_2 particles into the casting solution using NMP as solvent, and investigated their antibacterial, photocatalytic and antifouling properties. The results showed that the TiO_2 addition significantly affects pore size and hydrophilicity of the membrane and thus improves water flux of the modified PVDF/TiO_2 membrane. Application of DMAc as solvent for preparation of composite PVDF/TiO_2 membranes has been also investigated by Song *et*

Table 1 Properties and performance of flat sheet composite PVDF/TiO$_2$ membranes prepared in previous researches

PVDF (wt.%)	Solvent	TiO$_2$ Amount (wt.%)	Pore forming agent	Support	Pure water flux (l/m^{2}h.bar)	BSA Rejection (%)	Contact angle (°)	Porosity (%)	Ref.
15	NMP	0	-	Polyester nonwoven fabric	303	93	86.7	Not mentioned	Bae and Tak 2005
		0.3[a]			331	95	81.1		
10	NMP	0	-	Non-woven sheet	481.48	Not mentioned	89.1	Not mentioned	Damodar et al. 2009
		1			838.71		82.2		
		2			494.30		86.1		
		4			318.63		87.6		
12	NMP	0	-	PET nonwoven fabric	390	Not mentioned	80	Not mentioned	Oh et al. 2009
				PET film	310		72.5		
		2		PET nonwoven fabric	290		69		
				PET Film	300		68		
24	NMP	0	PEG 400	PE nonwoven fabric	37.5	0.1225[b]	79.4	Not mentioned	Bian et al. 2011
		0.1			50	0.1207[b]	77.2		
		0.25			60	0.1339[b]	73.5		
		0.35			95	0.1228[b]	72.1		
		0.5			120	0.1237[b]	71.6		
16	DMF	0	PEG	Polyester nonwoven fabric	88.2		78	Not mentioned	Cao et al. 2006
		< 2% 28 nm			107.3		84		
		< 2% 10 nm			111.7		76		
18	DMAc	0	PVP	No	155	52.3	82.8	63.3	Li et al. 2013
		5[c]			203	62.6	65.9	67.8	
		10[c]			237	70.6	59.7	74.1	
		12[c]			206	60.8	61.6	73.9	
12	DMAc	0	PEG 600		260	78[d]	78	Not mentioned	Song et al. 2012
		0.25			274	83[d]	-		
		0.5			232	81[d]	74		
		1			260	82[d]	-		
		1.5			282	79[d]	-		
		2			315	75[d]	-		
18	DMAc	0		Polyester sheet	76.99	99.9[f]		64.53	Ngang et al. 2012
		1.5[e]			392.81	96[f]		65.13	

[a] TiO$_2$/PVDF; [b] pore size (μm); [c] vol.% of the prepared solution for TiO$_2$;
[d] SDS-MB; [e] Anatase TiO$_2$; [f] pepsin

al. (2012) and Li *et al.* (2013) using PEG600 and PVP as pore forming agent, respectively (see rows 6 and 7 of Table 1).

A summary of similar studies on PVDF/TiO$_2$ composite flat sheet membranes is illustrated in Table 1.

As concluded from Table 1, the addition of TiO$_2$ to the casting solution can improve the antifouling properties of PVDF membranes but there is not any study regarding the suitable concentration of TiO$_2$ in the casting solution which contains mixed solvents. So further research works are still needed to determine the suitable formulation for PVDF/TiO$_2$ composite membranes.

Indeed, it seems that the advantageous of mixed solvents can be coupled with that of TiO$_2$ to improve the membranes hydrophilicity. However, to our best knowledge, there is no information about how TiO$_2$ nanoparticles influence morphology and performance of the mixed-solvent composite PVDF membranes.

In this study, the role of TiO$_2$ nanoparticles was investigated in preparation of mixed solvents PVDF membranes. Mixtures of DMAc and TEP were selected based on the results of some previous studies which showed a relatively acceptable performance for the prepared PVDF membranes (Tao *et al.* 2013, Li *et al.* 2010). Different techniques such as SEM, EDS, contact angle measurements and filtration experiments of water and BSA were applied to evaluate the morphology and performance of membranes.

2. Experimental

2.1 Materials

Polyvinylidene fluoride (PVDF) powder (Solef 1015, Solvay, France) was used as base polymer. N,N −dimethylacetamide (DMAc, ≥ 99.0) and triethylphosphate (TEP, > 98.0%) as solvents were obtained from Sigma Aldrich and Merck (Germany), respectively. Polyethylene glycol (PEG, MW = 200 Da) as pore forming agent was supplied by Merck (Germany). TiO$_2$ nanoparticles (with average size of 20-30 nm) and Bovine serum albumin (BSA, MW = 67,000 g/mol) were purchased from Sigma Aldrich. Deionized (DI) water was used throughout the experiments.

2.2 Membrane preparation

2.2.1 The effect of mixed solvent

In order to investigate the effect of TEP/DMAc mixing ratio, the flat PVDF membranes were prepared via immersion precipitation. To prepare the casting solution, the pore forming agent (PEG200) at a fixed amount of 5 wt.%, was added to a mixture of two solvents TEP and DMAc with different ratios as shown in Table 2 and mechanically stirred to mix completely. Then, PVDF powder (15 wt.%) which had been dried at 100°C for 24 h was added and each casting solution was mechanically stirred at 200 rpm for at least 12 h at 60-70°C to guarantee complete dissolution of the polymer. The casting solutions were cast onto a glass plate at 25°C by means of a casting knife with a gap of 250 μm, and then immersed into a coagulation bath (deionized water at 25°C) immediately. After complete coagulation during 3 h immersion in the bath, the membranes were transferred into a fresh water bath, which was refreshed frequently, to remove traces of the residual solvents, and then the prepared membranes were kept in deionized water until used.

Maryam Tavakolmoghadam, Toraj Mohammadi and Mahmood Hemmati

Table 2 Casting solution specification with different mixing ratios of the solvents

Rank	Membrane	PVDF (wt.%)	Solvent (wt.%)		PEG 200
			DMAc	TEP	
1	MTEP0	15	100	0	5
2	MTEP20	15	80	20	5
3	MTEP40	15	60	40	5
4	MTEP60	15	40	60	5
5	MTEP80	15	20	80	5
6	MTEP100	15	0	100	5

2.2.1.1 Calculation of the solubility parameters

Affinity of solvents to polymers can be estimated based on Hansen solubility parameters by introducing the solubility parameter (δ) which is defined as the square root of the cohesive energy density and describes the strength of attractive force between molecules. The solubility parameter (δ) of liquids and polymers can be defined as: (Wang *et al.* 2012)

$$\delta = \sqrt{\delta_d^2 + \delta_p^2 + \delta_h^2} \tag{1}$$

where, δ_d, δ_p and δ_h denote contributions of dispersive interactions (*d*), polar bonding (*p*) and hydrogen bonding (*h*), respectively.

The solubility parameter of mixed solvents can be calculated by eq. 2, based on volumetric average of the δ values of pure compounds: (Wang *et al.* 2012)

$$\delta_i = \frac{x_1 v_1 \delta_{i,1} + x_2 v_2 \delta_{i,2}}{x_1 v_1 + x_2 v_2}, \qquad i = d, p, h \tag{2}$$

where, δ_i is the solubility parameter of the mixed solvents, *x* is molecular fraction, and *v* is molecular volume, and 1 and 2 stand for the two solvents, respectively.

The smaller difference between the solubility parameters of polymer and solvent means the stronger dissolving capacity of the solvent and is calculated as

$$\delta_{p,s} = \sqrt{\left(\delta_{p,d} - \delta_{s,d}\right)^2 + \left(\delta_{p,p} - \delta_{s,p}\right)^2 + \left(\delta_{p,h} - \delta_{s,h}\right)^2} \tag{3}$$

Where *P* and *S* represent polymer and solvent. The solubility parameter values of the polymer and the solvents, are presented in Table 3.

2.2.2 TiO₂/PVDF composite membrane preparation

In order to prepare nanocomposite membrane TiO_2 nanoparticle contents were added to a fixed ratio of DMAc/TEP (40/60) and PEG200. For better distribution of TiO_2 nanoparticles in the membrane matrix, two sizes of test sieves (200 and 325, ASTM-E11) were used for mesh filtration of TiO_2 nanoparticles before adding to the casting solution. Certain amounts of TiO_2 nanoparticles according to Table 4 were added to the above mentioned solvents solution and sonicated in an ultrasonic bath for 30 min. Finally, PVDF powder (15 wt.%) which was dried at 100°C for 24 h

Table 3 Solubility parameters of PVDF and solvents

Component	δ_d MPa$^{1/2}$	δ_p MPa$^{1/2}$	δ_h MPa$^{1/2}$	δ MPa$^{1/2}$	δ_{PS} MPa$^{1/2}$
PVDF	17.2	12.5	9.2	23.17	-
DMAc	16.8	11.5	10.2	22.77	1.47
TEP	16.8	11.5	9.2	22.34	1.08
TEP/DMAc = (20/80)	16.93	11.5	9.42	22.53	1.35
TEP/DMAc = (40/60)	17.06	11.5	9.63	22.72	1.25
TEP/DMAc = (60/40)	17.18	11.5	9.83	22.89	1.16
TEP/DMAc = (80/20)	17.29	11.5	10.02	23.06	1.10

Table 4 TiO$_2$/PVDF membrane casting solution (composition and viscosity)

Membrane	PVDF (wt.%)	PEG200	DMAc/TEP	TiO$_2$ (wt.%)	Viscosity (Pa.s)
M0	15	5	40/60	0	16.1
M1	15	5	40/60	0.25	22.2
M2	15	5	40/60	0.5	35.2
M3	15	5	40/60	1	56.9

was added and each casting solution was mechanically stirred at 200 rpm for at least 24 h at 60-70°C to guarantee complete dissolution of the polymer. The casting procedure is the same as previously explained in Section 2.2.1. Viscosities of the casting solutions were measured using a Rheometer Measuring System (Anton Paar MCR501) at 25°C. This equipment uses the ramp stress test method, whereby a gradually increasing ramped stress is applied onto the sample solution, and the induced shear rate is continuously monitored. Viscosity of the sample solutions was calculated, based on the ratio of two parameters (i.e., shear stress versus shear rate). The reported data are viscosities at a shear rate of 10 s^{-1}.

2.3 Membrane characterization

2.3.1 SEM and EDS analysis
Morphology of the prepared membranes was characterized using a scanning electron microscope (SEM, TESCAN, Czech Republic). The membranes were cryogenically fractured in liquid nitrogen to observe their cross-sections. Both surface and cross-section of the membrane samples were sputter-coated with thin films of gold to make them conductive. The existence of TiO$_2$ and its content on the membrane surfaces were examined by Energy Dispersive X-ray Spectroscopy (EDS, VEGA3, TESCAN, Czech Republic).

2.3.2 AFM and surface roughness
The surface roughness of the membranes was characterized by an atomic force microscopy (SMENA-B, NT-MDT, Russia). The samples were cut into pieces of 3 cm by 3 cm and areas of 5 μm × 5 μm of each sample were scanned by non-contact mode.

2.3.3 Contact angle measurement

The contact angles formed by water droplets (4 μl) on the membrane surfaces were measured using sessile drop technique (OCA15 Plus, Dataphysics, Germany). The average of at least 5 measurements was reported.

2.3.4 Membrane porosity

The membrane porosity $\varepsilon(\%)$ was determined as a function of its dry-wet weight using the following equation

$$\varepsilon(\%) = \frac{m_w - m_d}{\rho_w A l} \times 100 \qquad (4)$$

where m_w is the weight of the wet membrane (g); m_d is the weight of the dry membrane (g); ρ_w is the water density (0.998 g·cm^{-3}), A is the area of membrane (cm^2) and l is the membrane thickness (cm) (Wang *et al*. 2012).

The membrane thickness was measured by an Electronic outside micrometer (Model 3109-25).

2.3.5 Filtration experiments

UF membranes were characterized by determination of pure water flux (J_{pw}), BSA rejection (R) and flux decline. A cross flow filtration setup as shown in Fig. 1 was used to measure pure water flux of the membranes and rejection measurement was carried out with aqueous solution of bovine serum albumin (BSA, MW = 67000, 300 mg L^{-1}) in phosphate buffer (0.1 M). Effective surface of the membranes was 33.3 cm^2. The membrane samples were initially compacted under pressure of 2 bar and at a cross flow velocity of 2 m/s with deionized water for 1 h before starting the filtration measurements. Pure water flux of each membrane samples was measured at a cross flow velocity of 1.25 m/s. All experiments were conducted at room temperature (25℃) and at a constant operation pressure of 1 bar. Pure water flux and BSA rejection were defined by Eq. (5) and (6), respectively.

$$J_{pw} = \frac{Q}{A \times T} \qquad (5)$$
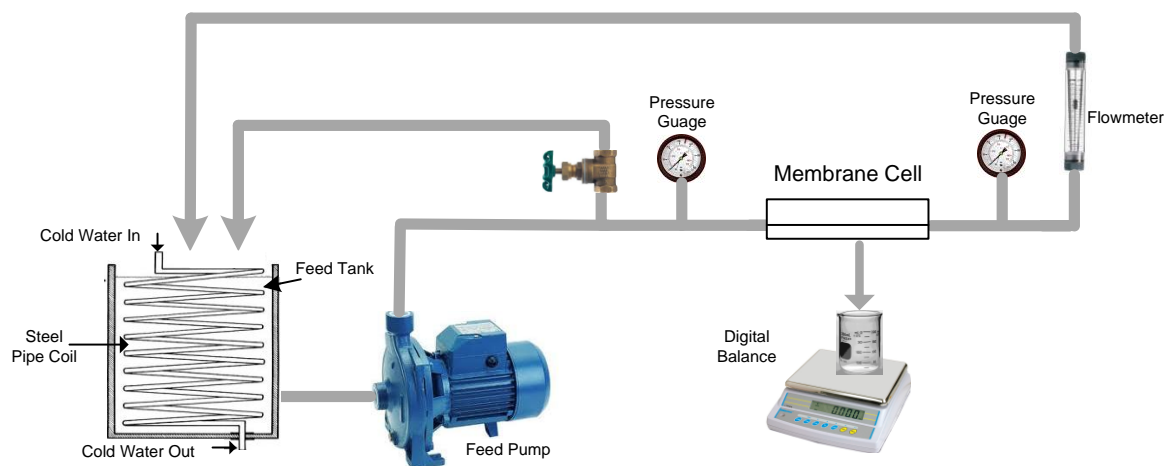
Fig. 1 Scheme of cross-flow filtration setup

$$\alpha = \left(1 - \frac{C_p}{C_F}\right) \times 100\% \tag{6}$$

where J_{pw} is pure water flux (L·h⁻¹ m⁻²), Q is volume of the permeated pure water (L), A is effective area of the membrane sample (m²), and T is permeation time (h). Also, α is BSA rejection (%), C_P and C_F are permeate and feed concentrations (wt.%), respectively.

BSA concentration was estimated using UV−visible spectrophotometry (Jasco-V670, Japan) at 280 nm.

2.3.6 Fouling analysis

To evaluate the antifouling property of the membranes, after pure water flux (J_{pw}) measurement, the feed tank was refilled with BSA solution (300 mg/L, pH = 7.4 in phosphate buffer) and BSA flux was measured (J_B) during 15 min. After 2 h of filtration, the membrane samples were washed using distilled water and finally pure water flux of the cleaned membranes was measured (J_{cw}).

To analyze the fouling process in detail, several equations were used to describe the fouling-resistant property of the membrane. The equations are as follows: (Rahimpour *et al.* 2011)

$$R_t(\%) = \frac{J_{pw} - J_B}{J_{pw}} \times 100 \tag{7}$$

Here, R_t is the degree of the total flux loss caused by total fouling. R_r and R_{ir}, described by Eqs. 8 and 9 show degree of flux loss caused by reversible and irreversible fouling, respectively

$$R_r(\%) = \frac{J_{cw} - J_B}{J_{pw}} \times 100 \tag{8}$$

$$R_{ir}(\%) = \frac{J_{pw} - J_{cw}}{J_{pw}} \times 100 \tag{9}$$

$$R_t = R_r + R_{ir} \tag{10}$$

In order to evaluate fouling resistant capability of the membranes, flux recovery ratio (FRR) was calculated using the following equation (Eq. (11))

$$FRR(\%) = \left(\frac{J_{cw}}{J_{pw}}\right) \times 100 \tag{11}$$

3. Results and discussion

3.1 The Effect of TEP/DMAc mixing ratio

Solvent plays a very important role in determining the ultimate membrane properties and performance. By mixing TEP and DMAc as solvent, PEG200 used as additive fixed at 5 wt.%, the effects of TEP/DMAc mixing ratio on the membrane morphologies and performances were
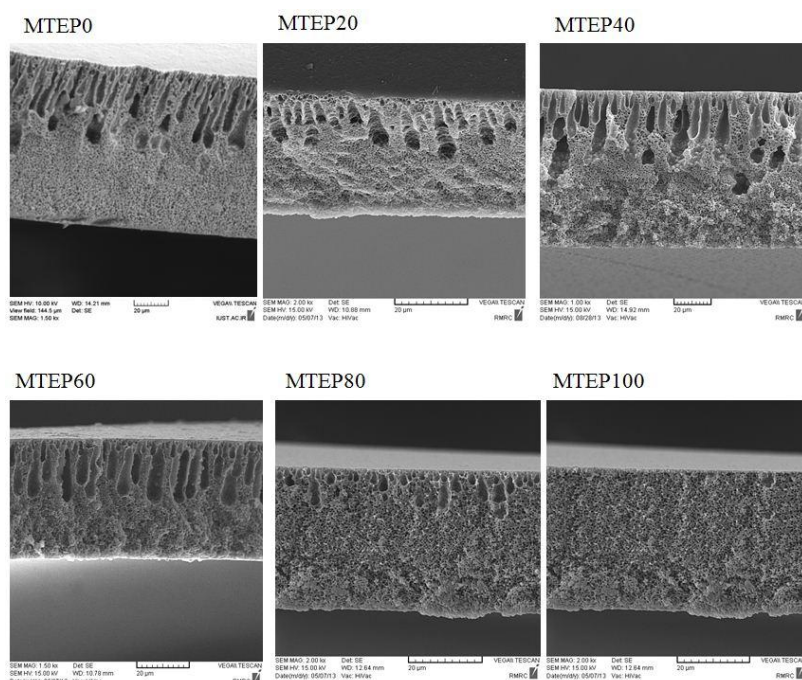
Fig. 2 SEM image of the prepared membrane using different mixed solvent

investigated. Cross sectional and top surface of the membranes cast with different mixing ratios of TEP-DMAc are shown in Fig. 2.

As illustrated, the membrane presents a typical asymmetric structure consisting of a thin dense top-layer and a thick porous sub-layer. The porous sub-layer itself consists of two separate parts of a finger-like and a sponge-like structure as it is also reported in previous researches (Bottino *et al.* 1991). Fig. 2 shows that, the fingerlike pores became wider with the increase of TEP content from 0 to 60 wt.% (MTEP0 to MTEP60) but then shortened as the content of TEP further increased from 60 to 100 wt.% (MTEP60 to MTEP100). It can be concluded that due to the faster rate of precipitation, by adding 60 wt.% of TEP to the mixed solvent, the macrovoids, becomes wider and extend to the middle part of the membrane. From the solubility parameters illustrated in Table 3, it seems there is an optimum value of solubility parameter for mixing solvents during casting solution of the systems in which Kinetic is dominant such as PVDF/DMAc-TEP. This phenomenon has been also observed in similar study for the mixture of DMAc and TMP (Li *et al.* 2010).

This is in consistence with the results illustrated in Figure 3 related to the pure water flux and porosity of the membranes with different ratios of DMAc/TEP.

Actually, by changing the solvent mixing ratio, thermodynamic and kinetic phenomena control the phase inversion and change the membrane morphology which can result in wider or shorter pores. The membrane morphology depends on the fact that either thermodynamic or kinetic phenomenon is dominant. Indeed the surface pore size also increases due to the thermodynamic stability as a result of the fact that less non-solvent is needed to induce phase inversion and cause instantaneous demixing and form larger surface pore size in MTEP60. Further increasing TEP, however, has opposite effect which results in reduced pore size and shorter fingerlike pores.
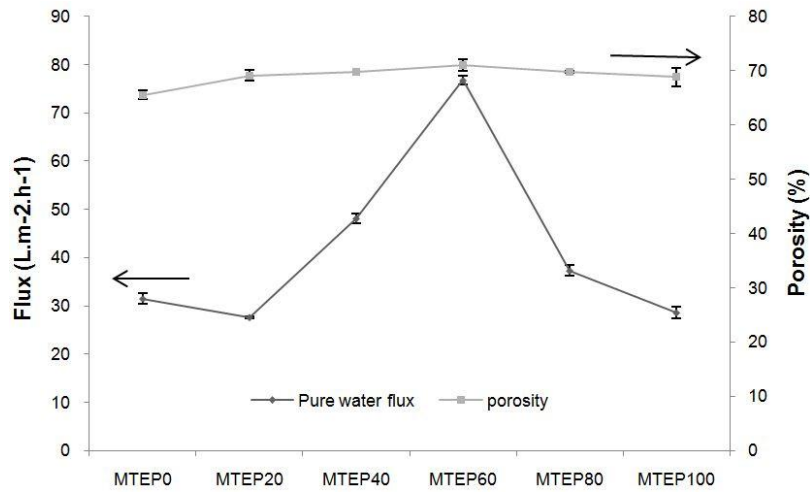
Fig. 3 Pure water flux of the membranes prepared using different solvent mixing ratios

It has been generally accepted that the morphology of microporous membrane affected by the precipitation rate influences the performances of the membrane.

As shown in Figure 3, the flux and the porosity of the membrane cast with TEP (60 wt.%)–DMAc (40 wt.%) (MTEP60) are the maximum amount, which are 76.8 Lm^{-2}h^{-1} and 78.09%, respectively. According to the aforementioned experiment results, the growing of macrovoids decreases permeation resistance and leads to the higher flux and porosity. However, as shown in Figure 4, the rejection of MTEP60 is not significantly different from that of others (MTEP0, MTEP20, MTEP40, MTEP80, and MTEP100), and equals to 82.46%; this result can be explained by the existence of macrovoids beneath the skin layer in all of the cross-section morphologies.

Therefore, the addition of 60 wt.% of phosphate in the mixed solvent is used in our further investigation on the effects of different mixed solvent on the membrane morphology and
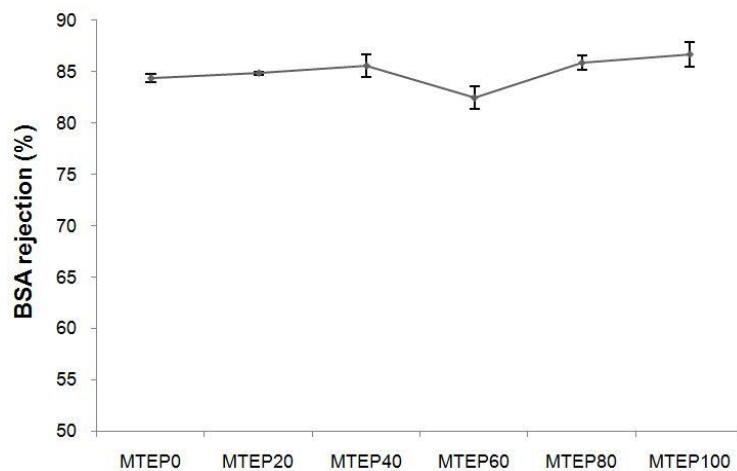

Fig. 4 BSA rejection of the membranes prepared using different solvent mixing ratios

$S_a = 69.02$
$S_q = 85.41$

(a)

$S_a = 24.94$
$S_q = 31.30$

(b)
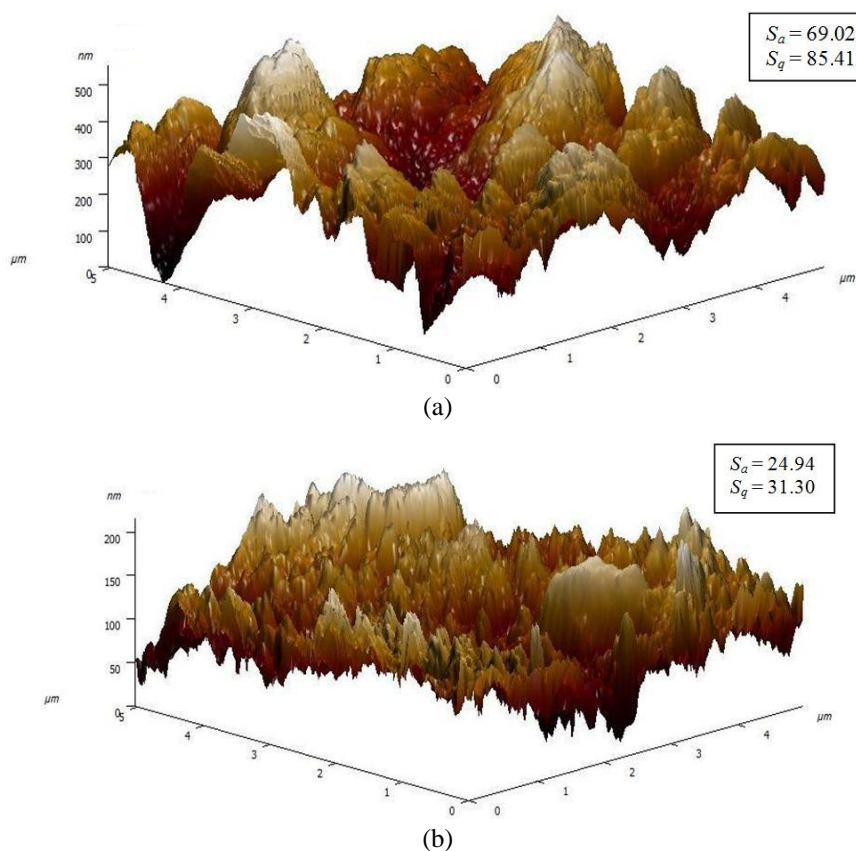
Fig. 5 AFM images of surface of a) membrane MTEP0 b) membraneMTEP60

performances, as discussed in the following investigations relating to the effect of TiO_2 nanoparticles on membrane morphology and performance. Surface roughness of the membrane MTEP60 were compared with the membrane prepared using single DMAc solvent and is shown in Fig. 5. As can be observed from the figure, using mixed solvent significantly reduced the surface roughness of the membranes.

3.2 TiO_2/PVDF composite membrane

3.2.1 Morphological study

To study the effect of TiO_2 nanoparticles on microstructure of the membranes, top surface and cross section SEM photographs of the PVDF/TiO_2 composite membranes were obtained as illustrated in Fig. 6.

TiO_2 entrapped membranes exhibit a more open structure with wider internal macrovoids. Comparing the three composite membranes with different amounts of TiO_2, formation of longer finger-like pores, which is caused by the faster precipitation process, is observed beneath the skin layer of M1. The elongation of this finger-like structure toward the bottom of the membrane decreases by increasing the TiO_2 content in the membrane casting dope solution.

This can be interpreted by the fact that the addition of TiO_2 not only increases water diffusion
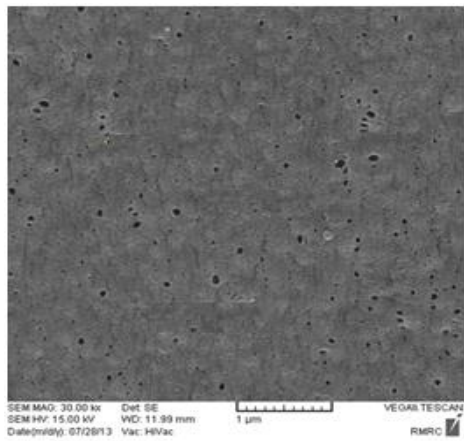
(a1)
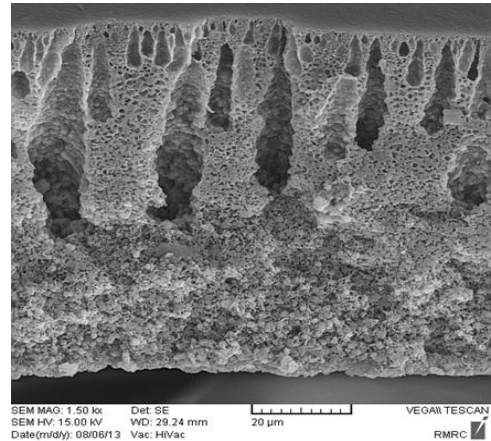
(b1)
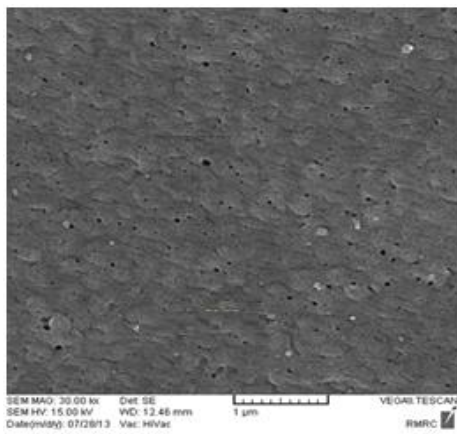
(a2)
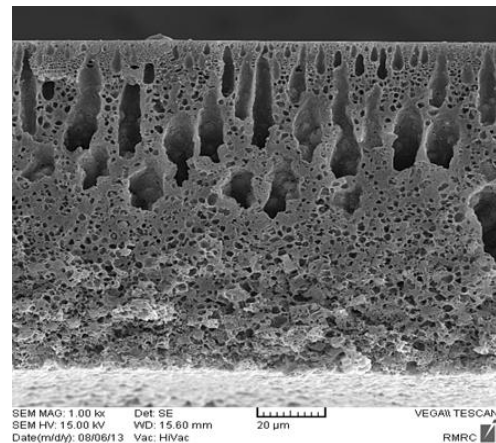
(b2)
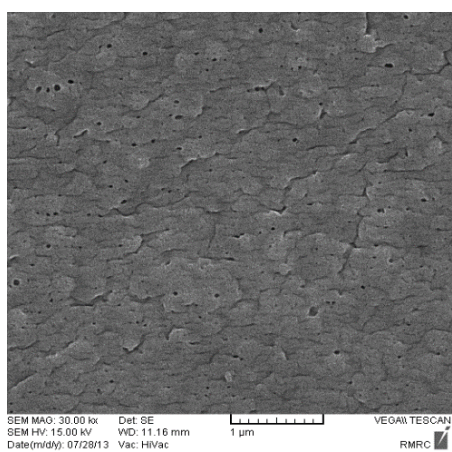
(a3)
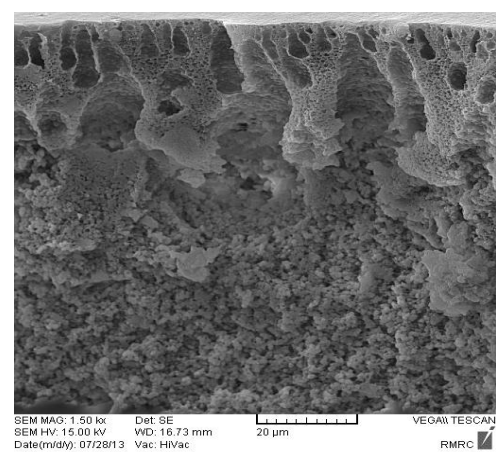
(b3)

Fig. 6 SEM images (a) surface; (b) cross section of composite membranes with (1) 0.25% TiO₂; (2) 0.5% TiO₂; (3) 1% TiO₂; (4) MTEP60
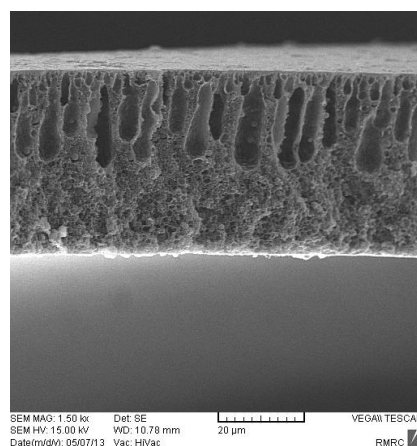
(b4)

Fig. 6 Continued

into the growing membrane due to its higher hydrophilic nature but also affects the interaction between polymer and solvent molecules by the hindrance effect of the particles (Arsuaga *et al.* 2013). By adding nanoparticles to the dope solution, thermodynamic stabilization of the system decreases. Thus, the system becomes less stable and leads to the quicker liquid-liquid phase separation with the more porous structure of cross-section (Zhang *et al.* 2013).

Application of low TiO_2 content less than 1 wt.% for better distribution of the nanoparticles in the membrane matrix is remarkable, in this study. However, as can be observed in Fig. 5, at higher contents of TiO_2, the membrane pores are plugged by the agglomerated particles during immersion precipitation and this shortens the finger-like pores beneath the skin surface of the membrane. This can adversely affect the membrane permeability as also reported in literature (Arsuaga *et al.* 2013). In other words, it is very important to use the suitable dosage of nanoparticles in the membrane casting solution since introduction of the higher content of nanoparticles may lead to a negative impact rather than an improvement.

3.2.2 Existence of TiO₂ on the composite membrane surface

Presence of the TiO_2 nanoparticles was investigated by energy dispersion of X-ray analysis (point EDS) confirming their existence on the top surface of the composite membranes. The surfaces of the membrane have been analyzed since it is more important to have an estimation of the TiO_2 nanoparticles on the surface to evaluate its degree of hydrophilicity which is inversely proportional to the extent of fouling in waste water treatment. The peak observed around 4.5 keV

Table 5 EDS composition of the composite membranes surface

| Sample	Weight percent of elements			
	C	O	F	Ti
M1	27.65	5.43	65.92	1.01
M2	26.99	5.96	64.82	2.23
M3	25.88	6.31	63.85	3.96
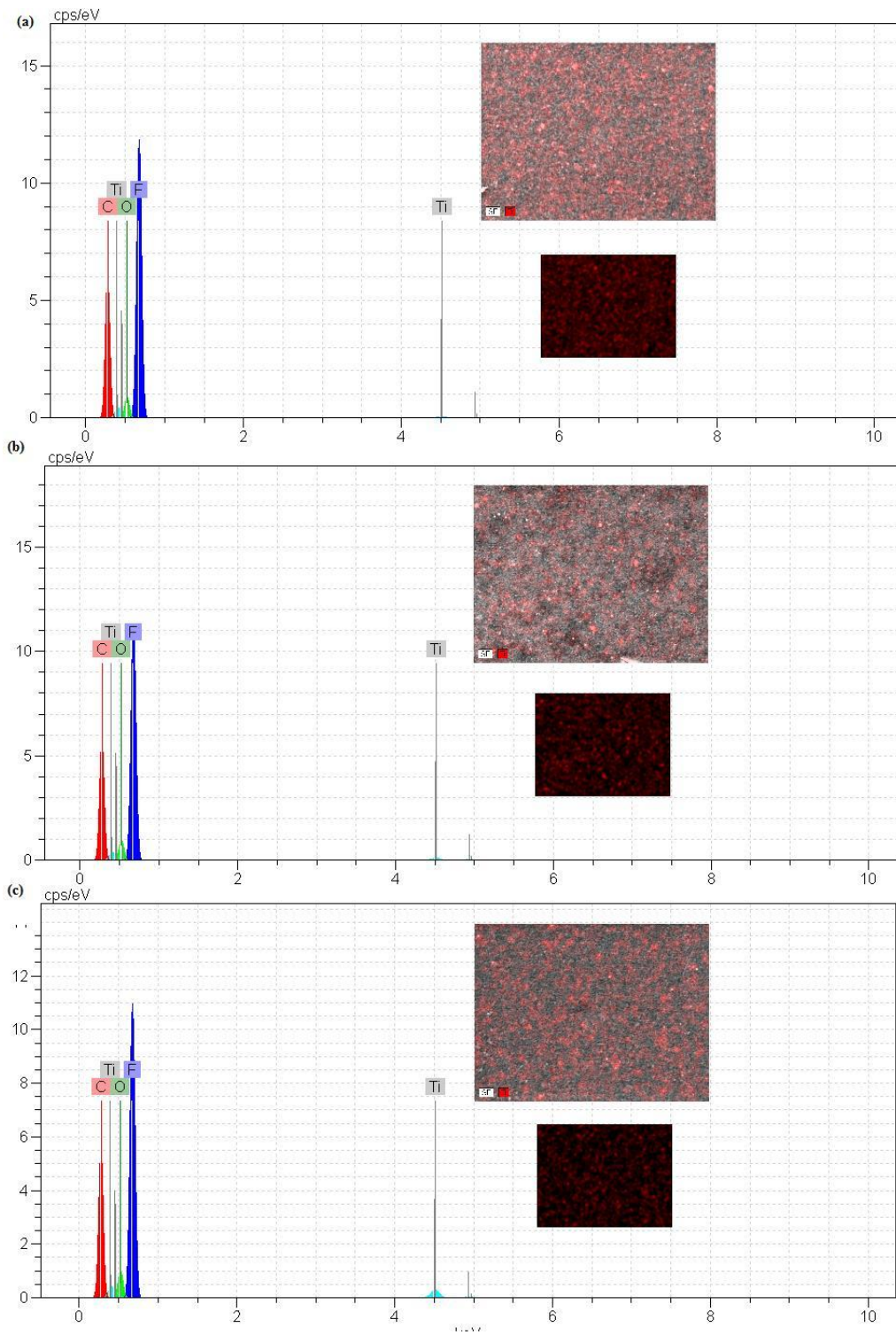
Fig. 7 EDS spectrum of composite membranes with a) 0.25% TiO$_2$, b)0.5% TiO$_2$, c)1%TiO$_2$

belongs to Ti and the peak around 0.7 keV belongs to Flour which comes from PVDF. The Ti peaks can be observed in the spectrum of the composite membrane as shown in Figs. 7(a)-(c) for each nanocomposite membrane. The EDS quantitative amounts of the elements for the three composite membranes are illustrated for comparison in Table 5.

As illustrated in Table 5, the presence of TiO_2 on the surface of the composite membranes has linearly proportional with the used amount. In other words, by increasing the TiO_2 content in the casting solution two times, its content on the membrane surface also increases twice. Less concentration of TiO_2 nanoparticles in the casting solution results in their less possible precipitation during the casting process and also solvent driven by the diffusive transfer can drag more nanoparticles towards the top of the membrane (Arsuaga *et al.* 2013). Considering that the former contents of TiO_2 in the casting solution were 0.25, 0.5 and 1 wt.%, the expected content of particles in the membrane structure should be around 1.63, 3.22 and 6.25 wt.%. Experimental calculation of TiO_2 weight percent based on the results illustrated in Table 5 confirmed that the particles were well dispersed in all cases. The calculated amount of TiO_2 based on EDX calculations are 1.68, 3.72 and 6.6 for M1, M2 and M3 membranes, respectively.

3.2.3 Sedimentation test

One of the reasons for inappropriate distribution of TiO_2 nanoparticles in polymeric membrane matrix is its relatively fast sedimentation rate of casting solution solvent suspension. Different physical or chemical methods have been reported to make more stable aqueous suspensions of TiO_2 while there is less information about the methods for stabilization of TiO_2 in organic solvents. Although, using dispersant may hinder the sedimentation of nanoparticles in the casting solution, however introducing any excess component into the polymeric membrane casting solution may influence the phase inversion process during membrane preparation. In this study, however, selection of the mixed solvent consisting triethyl phosphate and pore former agent (PEG) which act as dispersants resulted in more stable TiO_2 suspensions. It should be noted higher viscosity of TEP/DMAc mixture than single DMAc (0.99 in comparison with 0.94) is another reason for better distribution and delayed sedimentation of TiO_2 nanoparticles. This has been confirmed by visual comparison of sedimentation rate of two suspensions of TiO_2, one in DMAc and the other in a mixture of DMAc/TEP/PEG of the ratios we have used to prepare membrane casting solution as reported in Table 4. As shown in Fig. 8, the sedimentation test revealed that TiO_2 settled faster in pure DMAc compared with mixed solvent/PEG. Improved stabilization of TiO_2 in the casting solution leads to better distribution of nanoparticles in the membrane matrix.

3.2.4 Atomic force microscopy (AFM)

AFM analysis was used to investigate the effect of TiO_2 concentration bath on surface roughness of the PVDF membranes. Fig. 9 shows the three-dimensional surface AFM images of the prepared PVDF membranes. The roughness parameters for TiO_2 embedded and neat PVDF membranes are presented in Table 6. Roughness parameters (Sa, mean roughness and Sq, root-mean-square of Z data) were calculated using the AFM analysis software in an AFM scanning area of 5 μm $\times$ 5 μm. As illustrated in Fig. 9, the neat PVDF membrane had higher surface roughness than the modified membranes and the surface properties of membranes were strongly influenced by incorporation of TiO_2 nano-particles during phase inversion method. As illustrated, the mean roughness parameter of the PVDF first decreases to amount of 18.84 and then increases by further addition of TiO_2 nanoparticles due to agglomeration of excess nanoparticles on the membrane surface which results in rougher surface. However, the increment of M3 surface roughness is less

Fig. 8 Sedimentation test (a) just after sonication; (b) after 12 h: the left tube is TiO$_2$ in mixed solvent-PEG and the right is in DMAc

than M2, although, TiO$_2$ concentration is higher. So it can be concluded that although further incorporation of TiO$_2$ may increase the surface roughness, the inxcrement trend is not linear. This trend was also noticed to be due to settling of more amount of TiO$_2$ on the surface resulting in filling-in the valleys and less difference between ridge and valleys. The EDX mapping illustrated in Fig. 7 confirms this explanation (Safarpour *et al.* 2014).

3.2.5 Membrane hydrophilicity

Water contact angle for the neat PVDF-PEG membrane is relatively high (70.53°) indicating its less hydrophilic nature and this limits its application to separate hydrophobic solutes, due to the adsorption/desorption of organics on the membrane surface (Arsuaga *et al.* 2013).

As shown in Table 7, water contact angle of the PVDF membrane decreases with addition of TiO$_2$, implying that the hydrophilic characteristic of the incorporated TiO$_2$ nanoparticles makes the membrane surface more hydrophilic (Li *et al.* 2010). However, it should be noted that a little increase of contact angle amount was observed for M2 and M3 membranes due to their higher roughness. It is known that the contact angle value of a membrane of higher surface roughness is higher as compared to the other membrane of lower surface roughness, although both membranes are of similar hydrophilic nature (Rana and Matsuura 2010).

The remarkable result regarding this part is the relatively less contact angle (60.5°) of the composite membrane with low concentration of TiO$_2$ compared with the results of other similar studies by Song *et al.* 2012. They reported water contact angle of 74° for the membrane prepared using a similar casting solution containing 0.5 wt.% TiO$_2$, apart from using pure DMAc as a single solvent. It seems that applying the mixed solvents results in more improvement in hydrophilicity of the membranes. This can be due to better distribution of the TiO$_2$ nanoprtaicles in the polymer matrix and their better immigration towards the membrane surface as confirmed with EDS results.

3.2.6 Membrane porosity

In addition to the fingerlike and macrovoids growth (Fig. 6), which creates the larger voids into the polymeric membrane matrix, the inherent hydrophilic character of TiO$_2$ favors the water penetration into the polymer matrix. Both simultaneous effects could explain the higher porosity
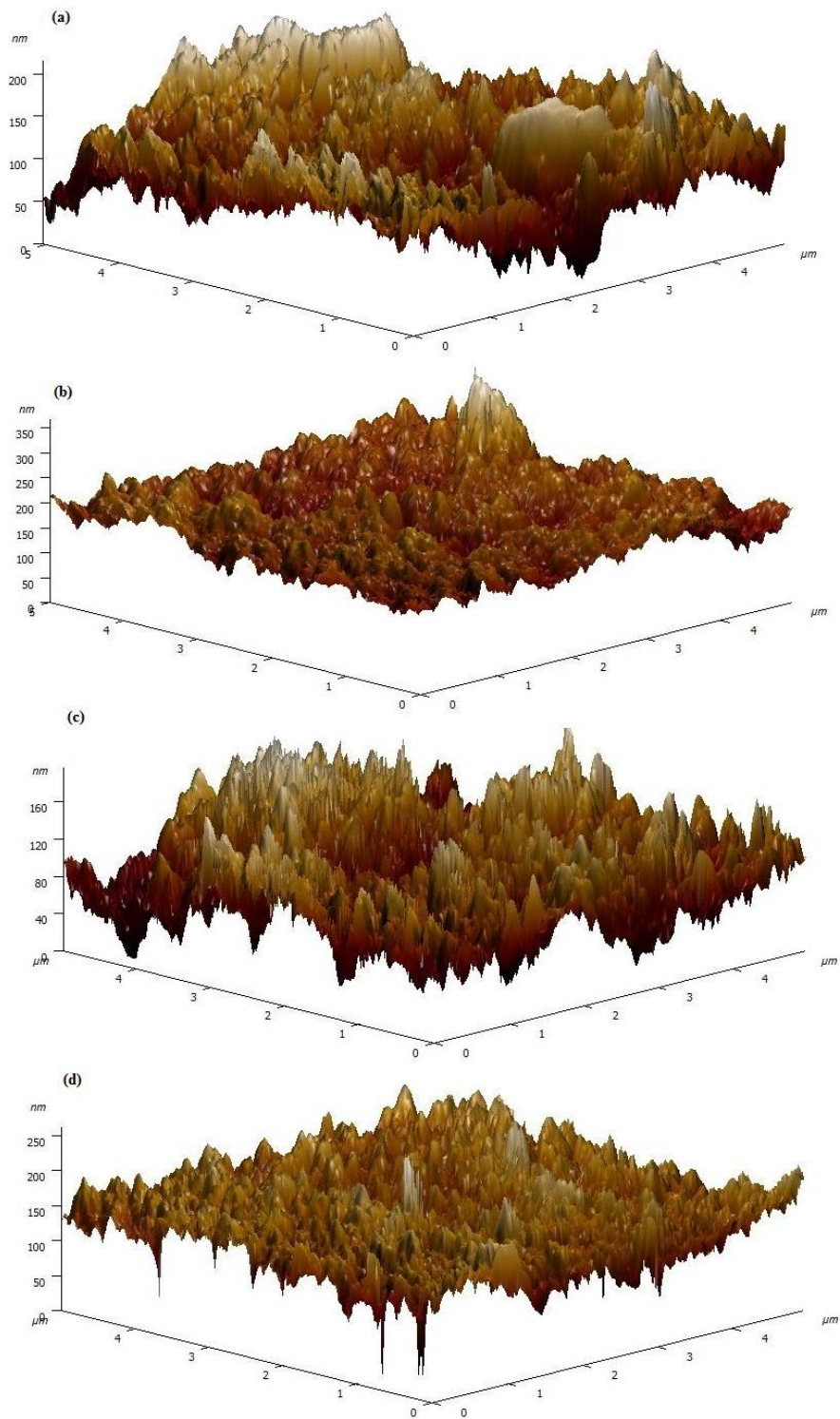
Fig. 9 AFM images of surface of (a) neat and composite PVDF membranes with; (b) 0.25% TiO$_2$; (c) 0.5% TiO$_2$; (d) 1% TiO$_2$

Table 6 Roughness parameters of the neat and TiO$_2$/PVDF composite membranes

Membrane	Average roughness, Sa	Root mean square, Sq
M0	24.96 ± 021	31.84 ± 0.41
M1	18.64 ± 0.43	24.73 ± 0.31
M2	22.37 ± 0.51	27.52 ± 0.33
M3	19.05 ± 0.36	27.17 ± 0.21

Table 7 Comparison of PVDF and composite membrane characteristics using DMAc and TEP as solvent

PVDF (wt.%)	Solvent	TiO$_2$ amount (wt.%)	Pore forming agent	Support	Pure water flux (l/m^{2}h.bar)	BSA Rejection (%)	Contact angle (^{o})	Porosity (%)	Reference
18	DMAc	0	-	Polyester fabric	37.7	98.08	67.56	-	Teow *et al.* 2012
15	TEP	0	-	-	1860	12 (0.27 μm)*	-	-	Tao *et al.* 2013
15	DMAc	0	PEG200		49.5	75.7		76.3	Li *et al.* 2010
	DMAc/TEP				64.6	90.1		76.1	
6	DMAc	0	-		87.7	-	83.8	33.7	Wang *et al.* 2013
	DMAc/TEP				89.6		84.9	44.2	
15	DMAc/TEP	0	PEG200	-	76.8	82.46	70.53	78.09	This study
		0.25			161.55	92.13	60.5	97.97	
		0.5			122.92	84.77	62.5	96.37	
		1			112.58	88.52	61	97.51	

observed for the modified membranes as shown in Table 7. Porosity of the neat membrane (78.09%) using the mixed solvents has not shown significant difference with the reported value (76.1%) by Li *et al.* 2010. The less porosity of M3 is due to pore blockage of the membrane by agglomeration of TiO$_2$ nanopartilces.

3.2.7 Filtration performance

As seen in Table 7, all of the composite membranes exhibited a higher pure water flux than the neat membrane, i.e., M1 membrane exhibits the highest value of 161.55 L m^{-2}h^{-1}. In general, as a consequent of porosity and hydrophilicity enhancement, the pure water flux increases significantly. It can be observed from the results that pure water flux reaches its maximum value at 0.25 wt.%., which is about two times higher than that of the neat membrane. This can be partially ascribed to an increment in the membrane porosity.

The enhancement of permeate flux is mainly attributed to the incorporation of TiO$_2$ which preferentially facilitate transport of water molecules (Li *et al.* 2013). However, when the TiO$_2$ loading is greater than 0.25 wt.%., the permeate flux of the PVDF/TiO$_2$ composite membrane decreases. It might be due to the fact that high content of TiO$_2$ nanoparticles produce highly viscous casting solution and this can be slow down the formation process of the composite

membrane, causing to form a thicker skin layer and a more compact network sub-layer that contains considerable the TiO_2 nanoparticles which can block the membrane pores (Kim and Van der Bruggen 2010) Therefore, it affects negatively the membrane permeability.

A comparison with similar literature results relating to the preparation of PVDF membranes using DMAc and TEP as solvent which is illustrated in Table 7 shows well the membrane performance improvement due to incorporation of the TiO_2 nanoparticles to the neat PVDF membrane prepared using the mixed solvents.

As can be observed in the table, using TEP can improves the pure water flux of the neat membrane and further modification of this membrane by incorporation of low content of TiO_2 can improve its permeability, while due to the presence of TEP more sponge like structure is formed according to the SEM image.

Performance of dynamic BSA fouling resistance was also investigated. The results in terms of BSA permeate flux relative to pure water flux (J_B/J_0) are described in Fig. 10. J_B/J_0 is the ratio of filtrate flux during the filtration process over the filtrate flux at the beginning of the filtration for each individual membrane. In general the permeate flux is declined gradually for the first 30 min of operation and then reaches its steady value. The composite membranes exhibit higher initial permeate flux values, with slightly less declined as time goes on as the result of less interactions between the BSA foulant and the membrane surface, as shown in Fig. 10. The flux decline values observed for the membranes are in agreement with their estimated hydrophilicity (contact angle) and roughness parameters as shown in Tables 6 and 7. The existence of TiO_2 nanoparticles on the membrane surface prevents the deposition/adsorption of BSA molecules on the membrane surface and in the pores and inhibits formation of a fouling layer, leading to a higher permeate flux. In other words, existence of TiO_2 nanoparticles on the membrane surface results in formation of a layer of chemisorbed H_2O on the surface. Such H_2O layer can absorb more water layer through van der Waals forces and hydrogen bonds. Formation of these layers of water prevents direct contact of the foulants on the membrane surface and consequently improves the antifouling ability. The water layers on the membrane surface prevents attachment of the foulants on the surface. Hence, it can be concluded that low membrane fouling rate in more hydrophilic surface can be attributed to lower adsorption rate of dissolved organics on the PVDF/TiO_2 membrane surface (Madeni *et al.* 2011, Tavakolmoghadam *et al.* 2016).

It can be observed that the steady BSA permeate flux for the neat membrane is declined to 40.4% of its initial flux due to the significant fouling potential of the feed. The corresponding values for the three composite membranes M1 and M2 are 80.6% and 76.9%., respectively. As observed, the extent of fouling reduces with incorporation of the TiO_2 nanoparticles.

The rejection potential of membranes was also explored, as shown in Table 7. As observed, the rejection increases due to the addition of TiO_2 nanoparticles in the casting solution. This phenomenon can be explained by the fact that the pores caused by adding nanoparticles were small enough to effectively prevent BSA molecules. At the same time, the surface of composite membrane was hydrophilic due to strongly bound water molecules that can occlude protein molecules from binding to surfaces (Song *et al.* 2012). In general, performance of the PVDF membrane improves in terms of the permeate flux maintaining the rejection. It is illustrated that low doping content is more effective than high TiO_2 nanoparticles lading in the casting solution (Song *et al.* 2012).

The stability of TiO_2 nanoparticles have been investigated by measurement of contact angle of the composite membranes after filtration tests. The results showed no significant change of contact angle values before and after the filtration which showed that most of the TiO_2 particles on the
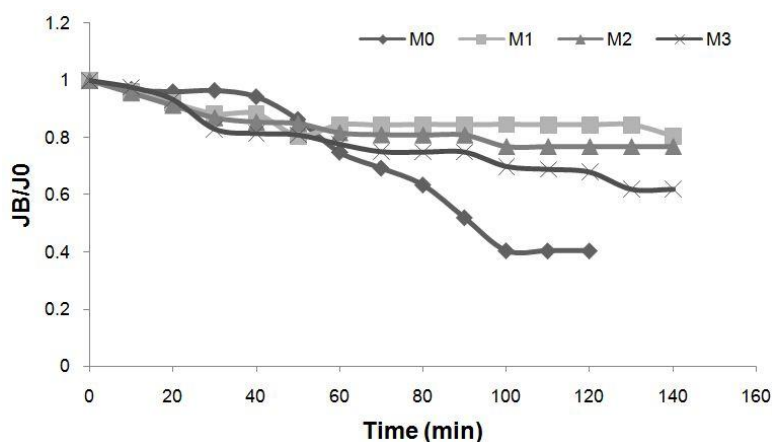
Fig. 10 Normalized BSA flux decline of the neat (M0) and composite membrane: M1 (0.25% TiO$_2$), M2 (0.5% TiO$_2$) M3 (1%TiO$_2$)

surface were stable.

3.2.7 Anti-fouling performance

The fouling resistance of the membranes containing the TiO$_2$ nanoparticles was also calculated for the BSA aqueous solution of 300 (mgL-1). Fig. 11 illustrates the effect of TiO$_2$ nanoparticle on the pure water and BSA flux of PVDF membranes prepared using mixed solvents. The pure water flux after cleaning of the membrane has been measured and shown in Fig. 11 which depicts the better flux recovery and cleaning of the composite membrane with 0.25% TiO$_2$ nanoparticles.

To evaluate the antifouling properties of the prepared membranes, fouling resistances of the neat and composite membranes were calculated as summarized in Table 8. As shown in the table, the flux recovery ratios (FRR) of composite membranes are significantly high compared to the neat membrane. In addition, the total flux losses of TiO$_2$ entrapped membranes are lower than neat
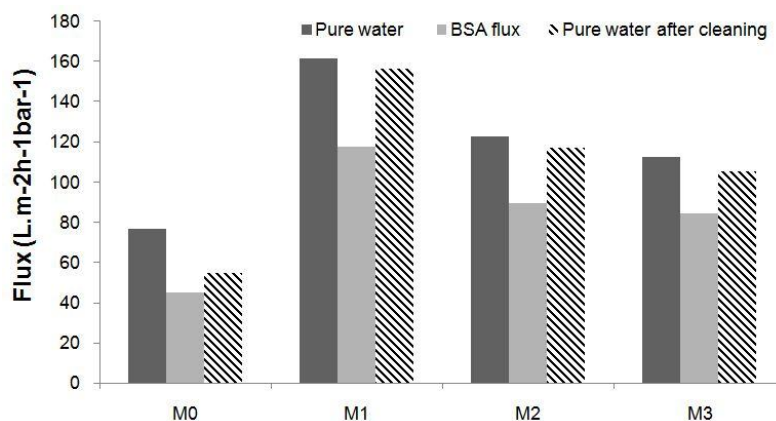

Fig. 11 Effect of TiO$_2$ addition on pure water and BSA flux of the neat (M0) and composite membrane: M1 (0.25% TiO$_2$), M2 (0.5% TiO$_2$) M3(1%TiO$_2$)

Table 8 Flux recovery and fouling resistance of the neat and composite membrane

Membrane	FRR (%)	R_r (%)	R_{irr} (%)	R_t (%)
Neat	71.80	13.33	28.20	41.52
M1	96.85	23.91	3.15	27.06
M2	95.4	22.57	4.6	27.17
M3	93.66	18.64	6.34	24.97

membrane. The degree of flux loss due to irreversible resistance (R_{ir}) for neat membrane is relatively high (28.2%) compared to the other membranes modified with TiO_2 (less than 7%).

The incorporation of TiO_2 nanoparticles mitigates considerably the hydrophobic interactions in the interface (organic foulants-membrane surface) that can lead to less hydrophobic layer formation (smaller R_r). In the case of M1 membrane, the degree of flux loss due to irreversible fouling resistance (R_{ir}) is diminished by more than 70% compared with the neat membrane. Therefore, it is evident that the higher number of hydrophilic centers (nanoparticles) in vicinity of the membrane surface avoids considerably the fouling layer formation. Previous investigation regarding the fouling mitigation effect of TiO_2 nanoparticles entrapped membranes using higher contents (between 2% and 4%) reported similar fouling resistance reduction (Damodar *et al.* 2012).

4. Conclusions

Composite PVDF/TiO_2 ultrafiltration membranes using mixed solvents (DMAc and TEP) were prepared and the effects of TiO_2 nanoparticles on the membrane morphology and performance have been studied. The results showed that applying lower than 1 wt.% of TiO_2 in the polymeric membrane matrix can mitigate the risk of agglomeration and this results in better distribution of nanoparticles and consequently more improvement in hydrophilicity. Indeed, using mixed solvents (DMAc/TEP) with lower content of TiO_2 nanoparticles (0.25 wt.%) affected the sedimentation rate of nanoparticles and consequently the distribution of nanoparticles in the casting solution and membrane formation which influenced the properties of the ultimate composite membranes. Degree of flux loss due to irreversible fouling resistance of the composite membrane reduced significantly and the flux recovery ratio (FRR) of 96.85% was obtained for the membrane prepared using DMAc/TEP mixing ratio of 40/60 and 0.25 wt.% TiO_2 nanoparticles.

References

Arsuaga, J.M., Sotto, A., Rosario, G., Martinez, A., Molina, S., Teli, S.B. and Abajo, J.d. (2013), "Influence of the type, size, and distribution of metal oxide particles on the properties of nanocomposite ultrafiltration membranes", *J. Membr. Sci.*, **428**, 131-141.

Bae, T.-H. and Tak, T.-M. (2005), "Effect of TiO_2 nanoparticles on fouling mitigation of ultrafiltration membranes for activated sludge filtration", *J. Membr. Sci.*, **249**(1-2), 1-8.

Bian, X., Shi, L., Yang, X. and Lu, X. (2011), "Effect of nano-TiO_2 particles on the performance of PVDF, PVDF-g-(Maleic anhydride), and PVDF-g-Poly(acryl amide) membranes", *Ind. Eng. Chem. Res.*, **50**(21), 12113-12123.

Bottino, A., Capannelli, G., Munari, S. and Turturro, A. (1988), "Solubility parameters of poly(vinylidene fluoride)", *J. Polym. Sci., Part B: Polym. Phys.*, **26**(4), 785-794.

Bottino, A., Camera-Roda, G., Capannelli, G. and Munari, S. (1991), "The formation of microporous polyvinylidene difluoride membranes by phase separation", *J. Membr. Sci.*, **57**(1), 1-20.

Cao, X., Ma, J., Shi, X. and Ren, Z. (2006), "Effect of TiO₂ nanoparticle size on the performance of PVDF membrane", *Appl. Surf. Sci.*, **253**(4), 2003-2010.

Damodar, R.A., You, S.-J. and Chou, H.H. (2009), "Study the self-cleaning, antibacterial and photocatalytic properties of TiO₂ entrapped PVDF membranes", *J. Hazard. Mater.*, **172**(2-3), 1321-1328.

Damodar, R.-A., You, S.-J. and Chiou, G.-W. (2012), "Investigation on the conditions mitigating membrane fouling caused by TiO₂ deposition in a membrane photocatalytic reactor (MPR) used for dye wastewater treatment", *J. Hazard. Mater.*, **203-204**, 348-356.

Guillen, G.R., Pan, Y., Li, M. and Hoek, E.M.V. (2011), "Preparation and Characterization of Membranes Formed by Non-solvent Induced Phase Separation: A Review", *Ind. Eng. Chem. Res.*, **50**(7), 3798-3817.

Kesting, R.E. (1985), *Synthetic Polymeric Membranes: A Structural Perspective*, John Wiley & Sons Inc., New York, NY, USA.

Kim, J. and Van der Bruggen, B. (2010), "The use of nanoparticles in polymeric and ceramic membrane structures: Review of manufacturing procedures and performance improvement for water treatment", *Environ. Pollut.*, **158**(7), 2335-2349.

Li, Q., Xu, Z. and Yu, L.Y. (2010), "Effects of mixed solvents and PVDF types on performances of PVDF microporous membrane", *J. Appl. Polym. Sci.*, **115**(4), 2277-2287.

Li, W., Sun, X.L., Wen, C., Lu, H. and Wang, Z. (2013), "Preparation and characterization of poly (vinylidene fluoride)/ TiO₂ hybrid membranes", *Front. Environ. Sci. Eng.*, **7**(4), 492-502.

Liu, F., Hashim, N.A., Liu, Y., Moghareh Abed, M.R. and Li, K. (2011), "Progress in the production and modification of PVDF membranes", *J. Membr. Sci.*, **375**(1-2), 1-27.

Loeb, S. and Sourirajan, S. (1964), High flow porous membranes for separating water from saline solutions; U.S. Pat. No. 3,133,132.

Luo, M.L. and Zhao, J.Q., Tang, W. and Pu, C.S. (2005), "Hydrophilic modification of poly(ether sulfone) ultrafiltration membrane surface by self-assembly of TiO₂ nanoparticles", *Appl. Surf. Sci.*, **249**(1-4), 76-84.

Madaeni, S.S., Zinadini, S. and Vatanpour, V. (2011), "A new approach to improve antifouling property of PVDF membrane using in situ polymerization of PAA functionalized TiO₂ nanoparticles", *J. Membr. Sci.*, **380**(1-2), 155-162.

Mulder, M. (1996), *Basic Principles of Membrane Technology*, Kluwer Academic Publishers, Dordrecht, The Netherlands.

Ngang, H.P., Ooi, B.S., Ahmad, A.L. and Lai, S.O. (2012), "Preparation of PVDF–TiO₂ mixed-matrix membrane and its evaluation on dye adsorption and UV-cleaning properties", *Chem. Eng. J.*, **197**, 359-367.

Oh, S.J., Kim, N. and Lee, Y.T. (2009), "Preparation and characterization of PVDF/TiO₂ organic–inorganic composite membranes for fouling resistance improvement", *J. Membr. Sci.*, **345**(1-2), 13-20.

Wang, Q., Wang, Z. and Wu, Z. (2012), "Effects of solvent compositions on physicochemical properties and anti fouling ability of PVDF microfiltration membranes for wastewater treatment", *Desalination*, **297**, 79-86.

Rahimpour, A., Madaeni, S.S., Taheri, A.H. and Mansourpanah, Y. (2008), "Coupling TiO₂ nanoparticles with UV irradiation for modification of polyethersulfone ultrafiltration membranes", *J. Membr. Sci.*, **313**(1-2), 158-169.

Rahimpour, A., Jahanshahi, M., Rajaeian, B. and Rahimnejad, M. (2011), "TiO₂ entrapped nano-composite PVDF/SPES membranes: Preparation, characterization, antifouling and antibacterial properties", *Desalination*, **278**(1-3), 343-353.

Rana, D. and Matsuura, T. (2010), "Surface Modifications for Antifouling Membranes", *Chem. Rev.*, **110**(4), 2428-2471.

Razmjou, A. (2012), "The effect of TiO₂ nanoparticles on the surface chemistry, structure and fouling performance of polymeric membranes", Ph.D. Dissertation; The University of New South Wales, Sydney, Australia.

Razzaghi, M.H., Safekordi, A., Tavakolmoghadam, M., Rekabdar, F. and Hemmati, M. (2014),

"Morphological and separation performance study of PVDF/CA blend membranes", *J. Membr. Sci.*, **470**, 547-557.

Safarpour, M., Khataee, A. and Vatanpour, V. (2014), "Preparation of a novel polyvinylidene fluoride (PVDF) ultrafiltration membrane modified with reduced graphene oxide/titanium dioxide (TiO_2) nanocomposite with enhanced hydrophilicity and antifouling properties", *Ind. Eng. Chem. Res.*, **53**(34), 13370-13382.

Shih, H.C., Yeh, Y.S. and Yasuda, H. (1990), "Morphology of microporous poly(vinylidene fluride) membranes studied by gas permeation and scanning electron microscopy", *J. Membr. Sci.*, **50**(3), 299-317.

Shon, H.K., Puntsho, S., Vigneswaran, S., Kandasamy, J., Kim, J.B., Park, H.J. and Kim, I.S. (2010), "PVDF-TiO_2 Coated Microfiltration Membranes: Preparation and Characterization", *Membr. Water Treat.*, *Int. J.*, **1**(3), 1-14.

Song, H., Shao, J., He, Y., Liu, B. and Zhong, X. (2012), "Natural organic matter removal and flux decline with PEG–TiO2-doped PVDF membranes by integration of ultrafiltration with photocatalysis", *J. Membr. Sci.*, **405-406**, 48-56.

Teow, Y.H., Ahmad, A.L., Lim, J.K. and Ooi, B.S. (2012), "Preparation and characterization of PVDF/TiO_2 mixed matrix membrane via in situ colloidal precipitation method", *Desalination*, **295**, 61-69.

Tavakolmoghadam, M., Mohammadi, T., Hemmati, M. and Naeimpour, F. (2016), "Surface modification of PVDF membranes by sputtered TiO_2: Fouling reduction potential in membrane bioreactors", *Desalin. Water Treat.*, **57**(8), 3328-3338.

Tao, M., Liu, F., Ma, B.R. and Xue, L.X. (2013), "Effect of solvent power on PVDF membrane polymorphism during phase inversion", *Desalination*, **316**, 137-145.

Wang, Q., Wang, Z. and Wu, Z. (2012), "Effects of solvent compositions on physicochemical properties and anti-fouling ability of PVDF microfiltration membranes for wastewater treatment", *Desalination*, **297**, 79-86.

Wang, P., Ma, J., Shi, F., Ma, Y., Wang, Z. and Zhao, X. (2013), "Behaviors and effects of differing dimensional nanomaterials in water filtration membranes through the classical phase inversion process: A review", *Ind. Eng. Chem. Res.*, **52**(31), 10355-10363.

Wu, G., Gan, S., Cui, L. and Xu, Y. (2008), "Preparation and characterization of PES/TiO_2 composite membranes", *Appl. Surf. Sci.*, **254**(21), 7080-7086.

Yeow, M.L., Liu, Y.T. and Li, K. (2004), "Morphological study of poly(vinylidene fluoride) asymmetric membranes: Effects of the solvent, additive, and dope temperature", *J. Appl. Polym. Sci.*, **92**(3), 1782-1789.

Zhang, P.-Y., Yang, H. and Xu, Z.-L. (2012), "Preparation of polyvinylidene fluoride (PVDF) membranes via nonsolvent induced phase separation process using a tween 80 and H_2O mixture as an additive", *Ind. Eng. Chem. Res.*, **51**(11), 4388-4396.

Zhang, G., Lu S., Zhang L., Meng, Q., Shen, C. and Zhang, J. (2013), "Novel polysulfone hybrid ultrafiltration membrane prepared with TiO_2-g-HEMA and its antifouling characteristics", *J. Membr. Sci.*, **436**, 163-173.

Zhang, Z., Guo, C., Liu, G., Li, X., Guan, Y. and Lv, J. (2014), "Effect of TEP content in cooling bath on porous structure, crystalline and mechanical properties of PVDF hollow fiber membranes", *Polym. Eng. Sci.*, **54**(9), 2207-2214.

ED

Nomenclature

δ	Hansen Solubility parameter
δ_d	Hansen Solubility parameter representing Dispersive interactions (d)
δ_p	Hansen Solubility parameter representing Polar bonding (p)
δ_h	Hansen Solubility parameter representing Hydrogen bonding (h)
x	Mole fraction
v	Mole volume
ε	Membrane porosity
m_w	Weight of the wet membrane (g)
ρ_w	Water density
A	Area of membrane (cm^2,m^2)
l	Thickness of membrane (cm)
J	Permeation flux (L h^{-1} m^{-2})
Q	Volume of the permeated pure water (L)
T	Permeation time (h)
α	BSA rejection (%)
C	Solute concentration wt.%
J_i	Initial permeate flux (L h^{-1} m^{-2})
J_{PW}	Pure water flux (L h^{-1} m^{-2})
J_B	BSA flux
J_{cw}	Pure water flux of the cleaned membranes (L h^{-1} m^{-2})
R_r	Degree of flux loss caused by reversible fouling (%)
R_{ir}	Degree of flux loss caused by irreversible fouling (%)
R_t	Degree of the total flux loss caused by total fouling (%)
FRR	Flux recovery ratio (%)

Indices

P	Polymer
S	Solvent
NS	Non-solvent
p	Permeate
r	Retentate